Physical and Electrochemical Characterizations of Poly(vinylidene fluoride-*co*-hexafluoropropylene)/SiO$_2$-Based Polymer Electrolytes Prepared by the Phase-Inversion Technique

Kwang Man Kim, Nam-Gyu Park, Kwang Sun Ryu, Soon Ho Chang

Ionics Devices Team, Basic Research Laboratory, Electronics & Telecommunications Research Institute, 161 Gajong, Yusong, Daejon 305-350, South Korea

ABSTRACT: Highly porous poly(vinylidene fluoride-*co*-hexafluoropropylene) (PVdF–HFP)-based polymer membranes filled with fumed silica (SiO$_2$) were prepared by a phase-inversion technique, and films were also cast by a conventional casting method for comparison. *N*-Methyl-2-pyrrolidone as a solvent was used to dissolve the polymer and to make the slurry with SiO$_2$. Phase inversion occurred just after the impregnation of the applied slurry on a glass plate into flowing water as a nonsolvent, and then a highly porous structure developed by mutual diffusion between the solvent and nonsolvent components. The PVdF–HFP/SiO$_2$ cast films and phase-inversion membranes were then characterized by an examination of the morphology, thermal and crystalline properties, absorption ability of an electrolyte solution, ionic conductivity, electrochemical stability, and interfacial resistance with a lithium electrode. LiPF$_6$ (1M) dissolved in a liquid mixture of ethylene carbonate and dimethyl carbonate (1:1 w/w) was used as the electrolyte solution. Through these characterizations, the phase-inversion polymer electrolytes were proved to be superior to the cast-film electrolytes for application to rechargeable lithium batteries. In particular, phase-inversion PVdF–HFP/SiO$_2$ (30–40 wt %) electrolytes could be recommended to have optimum properties for the application. © 2006 Wiley Periodicals, Inc. J Appl Polym Sci 102: 140–148, 2006

Key words: nanoparticles; membrane; electrochemistry

INTRODUCTION

Polymer electrolytes based on poly(vinylidene fluoride) (PVdF) have been studied in various types of dried, gelled, and porous films (or membranes) and determined to have high ionic conductivity at room temperature and good mechanical strength. Poly(vinylidene fluoride-*co*-hexafluoropropylene) (PVdF–HFP) has also been used as a matrix material for electrolyte films of rechargeable lithium batteries because of its high solubility in organic solvents, lower glass-transition temperature, and reduced crystallinity. A PVdF–HFP film is generally weaker than PVdF in mechanical strength because of the amorphous nature of the hexafluoropropylene (HFP) constituent. To enhance the mechanical properties, some inorganic nanoparticles, such as fumed silica (SiO$_2$) and titania (TiO$_2$), have been introduced into the PVdF–HFP system. This study of particle-filled polymer electrolytes has also shown that a PVdF–HFP/SiO$_2$ (or TiO$_2$) electrolyte film has increased ionic conductivity (because of the large amount of liquid absorption),[1] decreased interfacial resistance with a lithium electrode (because of the solid-solvent role),[2] and effective lithium-ion transport.[3] Consequently, it has finally been confirmed that nanoparticles in a polymer–electrolyte system can play some useful role in forming particle networks into polymer bulk (particle dispersion), inhibiting the crystallization or reorganization of polymer chains (solid plasticizer), and interacting with lithium ionic species (solid solvent).

On the other hand, a phase-inversion technique using solvent and nonsolvent components simultaneously has been considered an effective way of obtaining highly porous PVdF[4–12] and PVdF–HFP[5,11,13–24] electrolyte membranes applicable to rechargeable lithium batteries. Phase-inversion membranes can be formed by immersion precipitation, in which competitive mutual diffusion between the solvent and nonsolvent occurs to yield highly porous structures. This method is very beneficial for obtaining a planned morphology by the modulation of preparation parameters such as the kinds of solvent and nonsolvent, their concentrations, and the

crystallinity of the polymer matrix.[25] However, the porous nature of a phase-inversion membrane may not directly lead to an increase in the electrolyte uptake and consequently in the ionic conductivity. This is because of multiphase interactions occurring within the membrane, such as phase separation between the electrolyte filling up the pores and the swelled polymer amorphous regions.[12] The determination of diffusion coefficients with a pulsed-gradient spin-echo NMR technique[6,7,10,11,14,15,20,22] is a very promising way of proving an ionic conduction mechanism, which is associated with pore structures such as the pore size, porosity, and tortuosity (or pore connectivity).

In this study, we prepared highly porous PVdF–HFP/SiO$_2$ membranes by combining the concepts of nanoparticle inclusion and phase inversion. N-Methyl-2-pyrrolidone (NMP) was used as a good solvent for the polymer, and water was used as a nonsolvent. The inclusion of nanoparticles was aimed at the enhancement of the mechanical strength as well as other effects associated with applicability to rechargeable lithium batteries. For comparison, we also prepared comparatively compact PVdF–HFP/SiO$_2$ films by a conventional casting method. Particular attention was paid to how the highly porous structure developed in the membrane by the control of the SiO$_2$ content and by the adoption of the phase-inversion method. Some basic characterizations of the morphology and thermal and crystalline properties revealed the differences in the porous structures of the cast film and phase-inversion membrane. The electrochemical properties, measured for the electrolyte-filled films and membranes, provided information on ionic conduction, electrochemical stability, and interfacial reactions with lithium electrodes. Some useful conditions for polymer electrolyte membranes applicable to rechargeable lithium batteries can be obtained through such characterizations.

EXPERIMENTAL

The PVdF–HFP and SiO$_2$ were a commercially available fluoro copolymer (KynarFlex 2801, Atofina Chemicals; 12 mol % HFP) and disilazane-treated SiO$_2$ (Cab-O-Sil TS-530, Cabot Co.), respectively. A viscous slurry was prepared by the mixing of PVdF–HFP and SiO$_2$ in NMP in a ratio of 1:9 (w/w) PVdF–HFP/NMP. The silica content was varied from 0 to 70 wt % on the basis of PVdF–HFP/SiO$_2$. It was very difficult to make a slurry with more than 60 wt % SiO$_2$ because overdosing nanoparticles produced a powderlike mass. Viscous slurries with 0–50 wt % SiO$_2$ were spread on a clean glass plate with a doctor blade apparatus with a gap of 300 μm. Phase-inversion membranes were obtained by the prompt immersion of the glass plate into a flowing-water bath and by the drying of the

precipitates under ambient conditions for 24 h. In the flowing-water bath, the polymer component in the slurry began to solidify because of the penetration of water molecules, whereas the solvent component was exuded into the flowing water. In addition, the membranes obtained by the phase-inversion process and dried under air did not contain any moisture, and this was confirmed by thermogravimetric analysis in the range of 25–200°C.

For comparison, cast films were also obtained by the drying of the slurries spread on a glass plate in a vacuum oven at 150°C for 12 h. Cast films with more than 40 wt % SiO$_2$ could not be obtained because of the easily collapsing property dominated by the particulate feature, whereas the phase-inversion membranes with the same amounts of SiO$_2$ easily formed self-supporting films with mechanical strength. The phase-inversion membranes had more room to occupy nanoparticles because of their porous nature than simply cast films. However, the cast films with compact structures were much thinner (20–40 μm) than the phase-inversion membranes (80–100 μm).

For the PVdF–HFP/SiO$_2$ cast films and phase-inversion membranes, surface and cross-sectional morphologies were observed with a JEOL JSM 5610 scanning electron microscope. The image magnifications were 20,000 and 5000× for the surface and cross-sectional views, respectively. The thermal properties were measured with a DuPont 2100 Thermal Analyst differential scanning calorimeter with a 910 cell base under the conditions of a heating run (25–250°C) at the scanning rate of 10°C/min and a subsequent cooling run (250–60°C) at −5°C/min. From the results, the thermal parameters [melting point (T_m), crystallization temperature (T_c), heat of fusion (ΔH_m), and heat of crystallization (ΔH_c)] were analyzed in terms of the SiO$_2$ content and preparation method of the PVdF–HFP/SiO$_2$ samples. The crystalline properties of the films and membranes were investigated with a Philips X'Pert Pro X-ray diffractometer equipped with a Cu Kα_1 target X-ray tube and a fast X-ray detector (X'Celerator).

An electrolyte solution of 1M LiPF$_6$ dissolved in a mixture of ethylene carbonate (EC) and dimethyl carbonate (DMC) (1:1 w/w) was used as a swelling liquid for the pieces (2 × 2 cm^2) of cast films and phase-inversion membranes to produce PVdF–HFP/SiO$_2$ polymer electrolytes. We measured the liquid uptake as a function of time by weighing the polymer electrolyte after the electrolyte solution was absorbed. The liquid uptake (%) was determined as follows: (W_2 − W_1) × 100/W_1, where W_1 and W_2 denote the weights of the polymer electrolytes before and after the electrolyte solution is absorbed, respectively.

A conductivity cell (2 × 2 cm^2) comprising two stainless steel electrodes on each side of the polymer electrolyte was used to obtain the ionic conductivity of

PVdF–HFP/SiO$_2$ polymer electrolytes, which was determined from complex impedance spectra obtained with a frequency response analyzer (HF 1225 gain-phase analyzer, Solartron) in the frequency range of 0.1 Hz to 100 kHz. The temperature dependence of the ionic conductivity was obtained over a range of 0–80°C. The ionic conductivity (σ) was calculated from the bulk resistance (R) with the relation $\sigma = l/(R \times A)$, where l and A are the thickness of the polymer electrolyte and the cell area, respectively.

Cyclic voltammetry was performed to investigate the electrochemical window of the PVdF–HFP/SiO$_2$ polymer electrolytes with a stainless steel electrode in a three-electrode cell (2×2 cm^2), in which lithium served as both counter and reference electrodes. A MacPile II potentiostat/galvanostat system was used at a scanning rate of 0.1 mV/s in the range of 0–5 V (vs Li/Li$^+$). In addition, the interfacial stability between the lithium and polymer electrolyte was examined as a function of time by the monitoring of the impedance of a blocking cell (2×2 cm^2) with two lithium sheets at room temperature.

RESULTS AND DISCUSSION

Morphology

Surface and cross-sectional images of cast films and phase-inversion membranes of PVdF–HFP/SiO$_2$ are shown in Figure 1. At first glance, the pore structure is more developed in the phase-inversion membranes than the cast films. The cast films are highly compact in both the surface and cross section, and the compactness seems to be enhanced as the SiO$_2$ content increases. Consequently, the uptake of the electrolyte solution is expected to be very low for the cast films in comparison with the phase-inversion membranes (shown later in Fig. 4), although some complexities may exist in the correlation between the liquid uptake and ionic conductivity (shown later in Fig. 5). The compactness of the cast films could be caused by the excellent solvation effect of NMP for PVdF–HFP, which produces a homogeneous polymer solution, and then by the substantial crystallization of the polymer chain in the center of SiO$_2$ as a nucleating agent. The effect of the SiO$_2$ nucleating agent can be more obviously seen in a high-content sample, such as a 30 wt % SiO$_2$ cast film, which has a no more roughened surface than those of films with less SiO$_2$.

The phase-inversion membranes have highly porous surfaces and cross sections with increasing SiO$_2$ content, but the porous nature gradually disappears with the domination of the particulate feature when 30 wt % is exceeded. For samples of low SiO$_2$ contents (<20 wt %), small pores with a ~1-μm average diameter are developed with a spongelike pattern in which a certain degree of tortuosity and higher liquid uptake

are expected. Mutual diffusion between NMP and H$_2$O molecules during phase inversion leads to this pattern of pores without suffering obstacles by the relatively small number of SiO$_2$ nanoparticles. As the SiO$_2$ content increases, however, the pores become smaller, with a sparse distribution, giving a brittle bulk membrane with a comparatively roughened surface. A great number of filler nanoparticles suspended with small interparticle distances play the role of inhibiting the formation of large pores during phase inversion. Many SiO$_2$ nanoparticles surrounded by the same mass no longer interact as nucleating agents, but they collapse among tiny crystallites that are slightly grown near SiO$_2$ nucleates to yield weak mechanical properties.

In comparison with the phase-inversion morphologies reported by others,[8,9,12,21,25] these membranes do not exhibit fingerlike images but show a spongelike morphology at low SiO$_2$ contents and then a brittle bulk state containing a range of pores distributed irregularly when 30 wt % SiO$_2$ is exceeded. It seems that the absence of a fingerlike cavity or asymmetric structure between the top and bottom layers of a phase-inversion membrane can be achieved by competitive mutual diffusion between NMP and water molecules on all sides of the membrane, which is peeled off from the glass plate just after immersion in flowing water. Some parameters that can determine this morphology can be considered: porosity and tortuosity (or pore connectivity),[21] which depend on the diffusion rates of water (penetrating) and NMP (escaping) in this situation. The flow rate in the water bath may also be a factor for adjusting the diffusion rates because it would help the fast removal of NMP and the fast introduction of water. In addition, SiO$_2$ in the phase-inversion process may play important roles in forming and stabilizing pores, enhancing the mechanical strength, and increasing the wettability with an electrolyte solution.[13] Excessive inclusion of SiO$_2$, however, eventually leads to difficulty in preparing a self-supporting polymer membrane because of the easily crushable feature by the overdosing of nanoparticles.

Thermal and crystalline properties

The addition of inorganic fillers such as SiO$_2$, Al$_2$O$_3$, and TiO$_2$ is known to contribute in general to the reduction of crystallinity in polymer films. This is not necessarily true in this case with the solvent NMP. Figure 2 and Table I show differential scanning calorimetry thermograms and thermal data, respectively, of PVdF–HFP/SiO$_2$ cast films and phase-inversion membranes. As the SiO$_2$ content increases, T_m slightly shifts up and down, but ΔH_m suffers an irregular pattern of increasing and decreasing in both the films and membranes. Fortunately, the effect of crystallinity changes with the addition of SiO$_2$ is comparatively
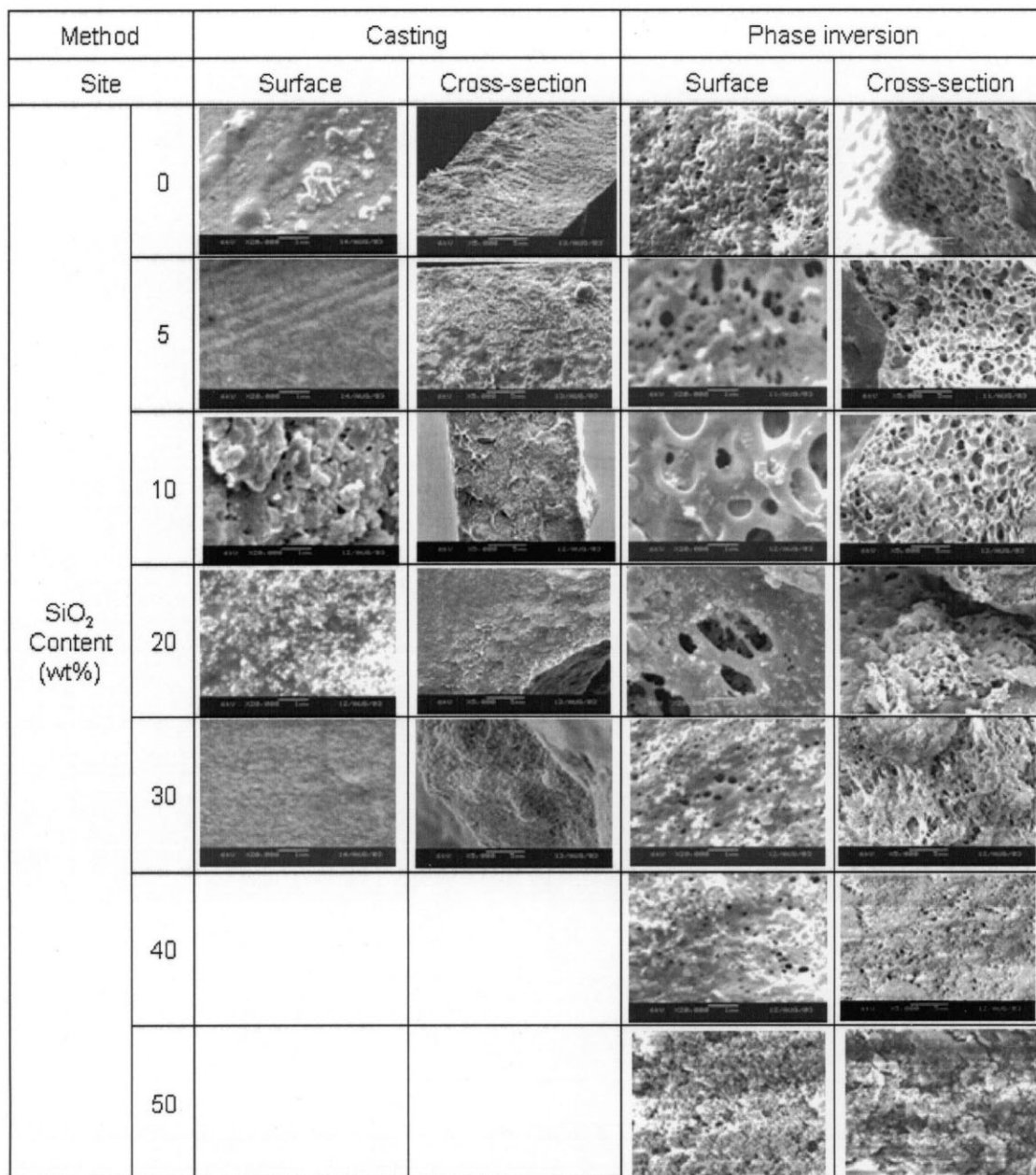
Figure 1 Scanning electron microscopy images of PVdF–HFP/SiO$_2$ films prepared by the casting and phase-inversion methods. The image magnifications are 20,000 and 5000× for the surface and cross-sectional views, respectively.

small because the absolute range of crystallinity (ca. 6–19% vs the 100% reference of pure α-phase PVdF crystal[26,27]) is small in comparison with other cases of using SiO$_2$/acetone (40–60%)[1] and TiO$_2$/acetone (20–60%).[2,3] We emphasize that the use of NMP as a solvent seems to give PVdF–HFP/SiO$_2$ with very low crystallinity, that is, a limited rearrangement of PVdF chains prohibited by solvent–polymer interaction (probably the interaction between the N atom of NMP and the vinylidene fluoride chain[28]).

On the other hand, cast films show a different melting behavior, in that a small, endothermic peak at 120–130°C appears before the melting of the main

crystalline phase (~144°C), whereas phase-inversion membranes have a broad melting peak over 120–160°C. The small, endothermic peaks for the cast films seem to be comparable to the melting of crystals after isothermal crystallization[29,30] and then probably correspond to dominant α-phase and minor γ-phase PVdF crystals.[29] Broad melting peaks for phase-inversion membranes seem to also be associated with the phase change of PVdF crystallites from the dominant α phase to the coexistence of α-, β-, and γ-phase crystals.[29]

A cooling run for the cast films produces slightly lower T_c values than the use of acetone as a solvent;[1]
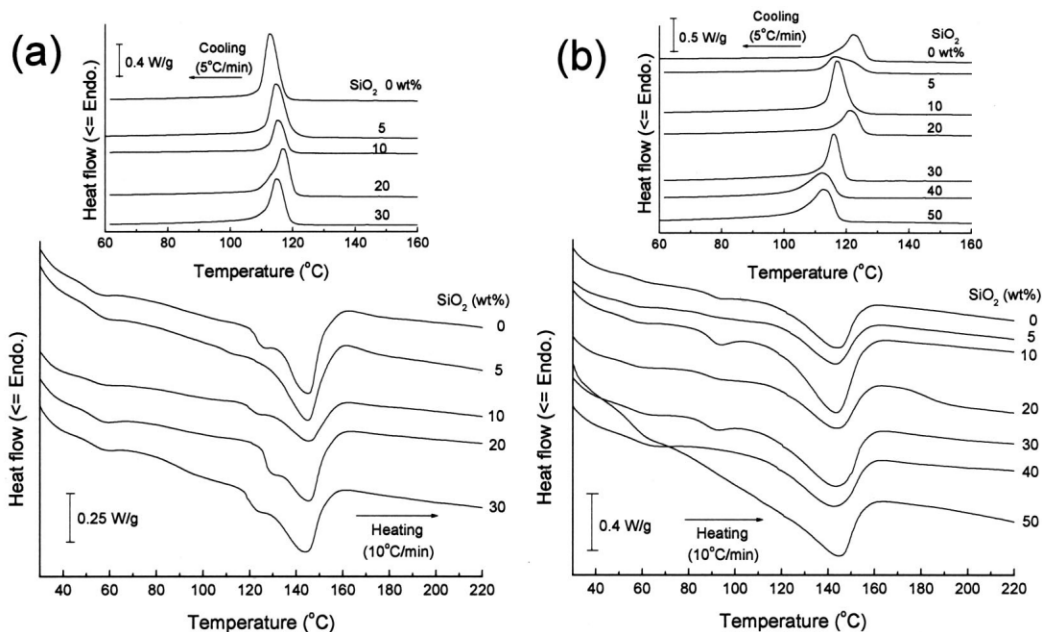
Figure 2 Differential scanning calorimetry thermograms of PVdF–HFP/SiO₂ films prepared by (a) casting and (b) phase-inversion methods. The small figures on top are the results of cooling runs at −5°C/min. The films were examined after heating runs from room temperature to 250°C at 10°C/min.

this is reflected by the delay of crystallization due to the difference in the interaction intensities of the solvent molecules and polymer in the melt state. Also, a slight increase (from 112 to 116°C) in T_c appears with increasing SiO₂ content, and this means that SiO₂ may act as a nucleating agent and then promote fast recrystallization. Thus, the cast films should have compact structures in both the surface and cross section. Phase-inversion membranes, however, show a small decrease (from 122 to 112°C) in T_c with increasing SiO₂ content; competitive mutual diffusion between the solvent and nonsolvent suppresses the role of the SiO₂ nucleating agent during the cooling run. Thus, the pore structure by mutual diffusion may be first formed, and then the weak crystal arrangement is completed. This may be a reason for the highly developed porous structure of the phase-inversion membranes, which depends on the relative diffusion rates

of the solvent and nonsolvent as well as the SiO₂ content in part.

The X-ray diffraction results in Figure 3 show that the addition of SiO₂ does not necessarily lead to a reduction of the crystallinity. The SiO₂ nanoparticles used here have in principle an amorphous nature that does not show any peak in the overall diffraction pattern, but it may change the peak intensity of the PVdF crystalline phase. For the cast film, the peak intensity at a low diffraction angle ($2\theta < 25°$) suffers a small decrease or increase with increasing SiO₂ content, but the intensity at a high angle ($2\theta = 38°$) corresponding to the PVdF $\alpha(131)$ phase[2,3,31] increases gradually. In comparison with the same case of using acetone as a solvent,[1] the intensity difference depends on the interaction between the solvent molecules and polymer chains.[28] For instance, the solvents containing $>C=O$ interact strongly with PVdF, reflecting the

TABLE I
Thermal Properties of PVdF–HFP/SiO₂ Cast Films and Phase-Inversion Membranes

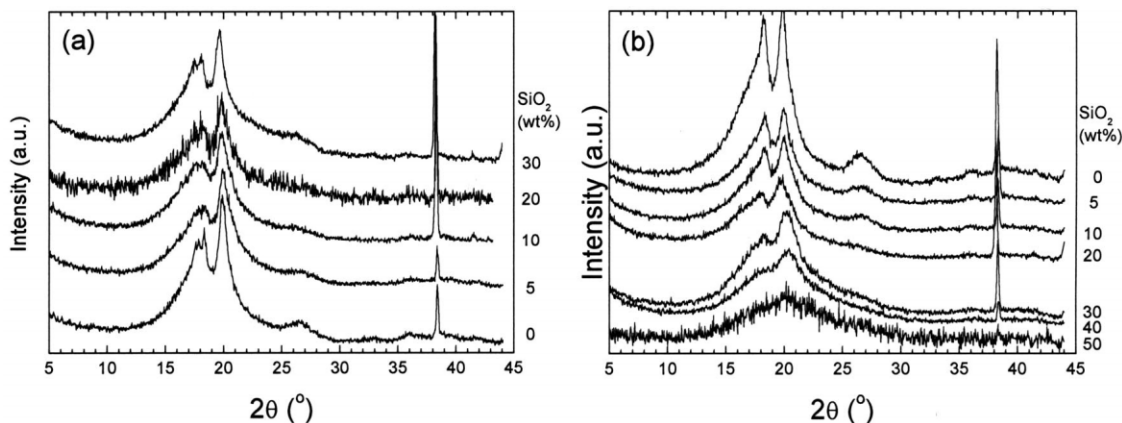| SiO₂ (wt %)	Cast film				Phase-inversion membrane			
	T_m (°C)	ΔH_m (J/g)	T_c (°C)	ΔH_c (J/g)	T_m (°C)	ΔH_m (J/g)	T_c (°C)	ΔH_c (J/g)
0	144.9	16.4	112.5	4.5	144.3	8.7	122.2	4.8
5	144.7	14.7	114.7	4.3	143.2	13.4	116.5	3.7
10	145.1	5.9	115.2	2.7	143.4	18.6	117.0	6.9
20	145.3	12.9	116.7	4.5	143.8	17.3	121.2	5.0
30	143.8	9.0	114.9	4.9	143.4	16.1	116.0	6.4
40					142.6	16.5	112.2	5.4
50					144.7	15.5	112.6	6.3

Figure 3 X-ray diffraction spectra of PVdF–HFP/SiO$_2$ films prepared by (a) casting and (b) phase-inversion methods.

diffraction intensities at a low angle,[28] whereas those containing >C=O and N atoms (e.g., NMP and dimethylacetamide) have low probability to interact and thus strengthen the intensity of the PVdF α(131) phase;[32] this is consistent with this case.

On the other hand, Figure 3(b) shows that in the phase-inversion membranes, the amorphous region is more emphasized than the crystalline phase formed by the rearrangement of the polymer chains, and this trend is enhanced with increasing SiO$_2$ content, which is reflected by the peak broadness. The phase-inversion PVdF–HFP/SiO$_2$ membranes suffer the changes of the crystal phase over the entire range of diffraction angles with increasing SiO$_2$ content, that is, for PVdF, α(020) at $2\theta = 18°$, α(110) at $2\theta = 20°$, α(021) or γ(022) at $2\theta = 26.5°$, and α(131) at $2\theta = 38°$.[30,31] Although the phase-inversion membranes have a highly developed porous structure (Fig. 1) with low crystallinity (9–18% in Table I), there exists a big deviation between the scales of the pore size and crystal phase. For example, the crystal size (L_{hkl}) determined from the Scherrer equation for PVdF is approximately 1–10 nm.[30] The crystal size changes do their work on small scales under low crystallinity, and thus there is no correlation between the porous structure and crystalline phase.

Liquid absorption and ionic conductivity

It may be understood that a phase-inversion membrane is expected to have more liquid uptake than a cast film because of its highly porous structure. As shown in Figure 4, a great amount of liquid absorption (maximum > 400%) occurs in the phase-inversion membranes, except for the sample with 50 wt % SiO$_2$. Liquid uptake of 200–400% for the membranes is very high in comparison with other PVdF–HFP/SiO$_2$ (or TiO$_2$) cast films.[1–3] Also in Figure 5, the membranes show higher ionic conductivity than the cast films over the temperature range of 0–80°C, except for the

sample with 5 wt % SiO$_2$. Such a trend between the liquid uptake and ionic conductivity, that is, a correlation that higher uptake leads to higher ionic conductivity, is just a general one, but somewhat complicated features can be possible in each case having a different pore structure and SiO$_2$ content. In particular, the phase-inversion membrane with 50 wt % SiO$_2$, showing a brittle morphology, behaves like a good ionic conductor by absorbing the liquid electrolyte a little; this is contrary to the correlation. This fact does not support the idea that the development of a pore structure leads to an increase in liquid absorption. In a similar way, it can also be said that all liquids absorbed do not necessarily contribute to ionic conduction. Ionic conduction in the phase-inversion membranes can be separated into more than two modes with respect to some factors such as the carrier migration, cavity (pore) barrier, and interaction with the swelled polymer.[10,11] Problems concerning the carrier
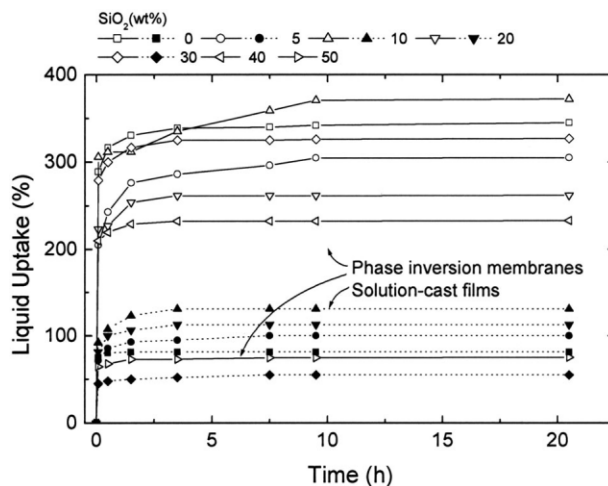

Figure 4 Liquid uptake of PVdF–HFP/SiO$_2$ films prepared by casting and phase-inversion methods. The electrolyte solution was 1M LiPF$_6$ dissolved in EC/DMC (1:1 w/w).
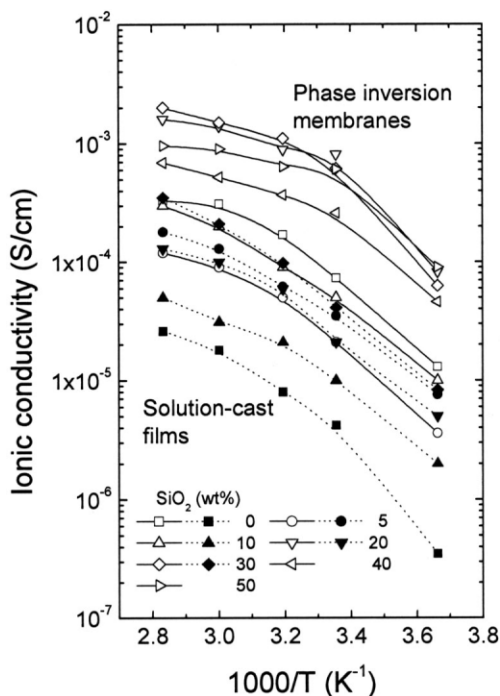
Figure 5 Arrhenius plot of the ionic conductivity of PVdF–HFP/SiO$_2$ electrolyte films prepared by casting and phase-inversion methods. The electrolyte solution was 1M LiPF$_6$ dissolved in EC/DMC (1:1 w/w).

migration or ionic conduction mechanism in these membranes should be solved by a further precise study, such as pulsed-field-gradient spin-echo NMR measurements[10,33] with cationic (^{7}Li) and anionic (^{19}F) probes. Also, another approach may be needed to explain the relationship between the liquid uptake and morphology in terms of the tortuosity or pore connectivity.[21]

Despite such contradictions, the phase-inversion membranes show room-temperature ionic conductiv-

ities ranging roughly from 10^{-4} to 10^{-3} S/cm, an adequate range for application to the polymer electrolyte of a rechargeable lithium battery. The temperature dependence of the ionic conductivity also shows empirical Vogel–Tammann–Fulcher behavior, which deviates from Arrhenius-type behavior, that the Li$^+$ conduction environment keeps constant in the temperature region. These polymer electrolytes provide different conduction behaviors with respect to temperature, that is, two Li$^+$ conduction modes in a liquid-like medium at elevated temperatures and in freezing solid solutions at low temperatures.

Electrochemical stability and interfacial resistance

The electrochemical windows of the PVdF–HFP/SiO$_2$ electrolytes containing 1M LiPF$_6$ and EC/DMC (1:1 w/w) are shown in Figure 6 as cyclic voltammograms. For the cast-film electrolytes, cathodic stability is achieved in the potential range of 0–5 V versus Li/Li$^+$, except for the small preoxidation wave from 3.5 V for the 30 wt % SiO$_2$ sample. This sample is also highly reactive by lithium-plating reduction in a low potential region (0–2.5 V), whereas others exhibit very small anodic peaks near 2 V, which have a maximum lithium-plating current density of 0.015 mA/cm^2. In contrast, the phase-inversion-membrane electrolytes have the same magnitude of anodic peaks at similar potentials, but nearly constant cathodic stability is observed with a very low current density (<0.005 mA/cm^2) over the potential range of 0–5 V versus Li/Li$^+$. Concerning the application to rechargeable lithium batteries, the phase-inversion membranes are expected to have more stable electrochemical windows than the cast films.

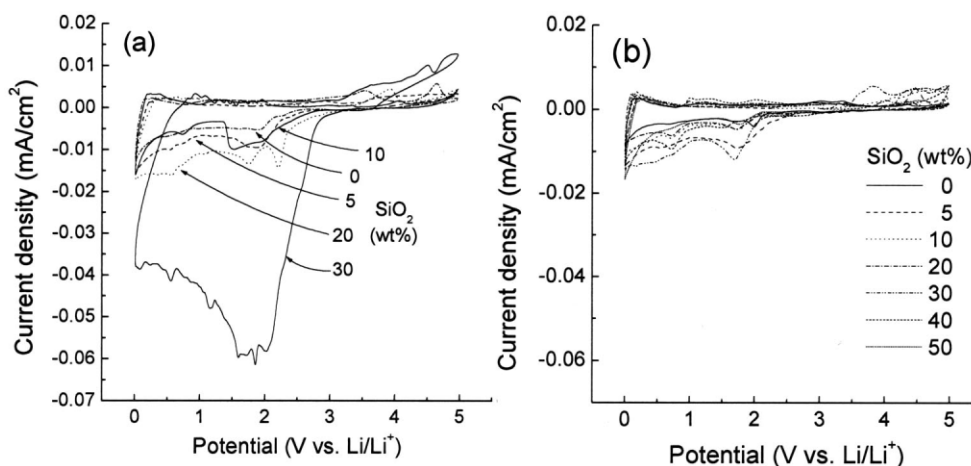Sample impedance spectra of PVdF–HFP/SiO$_2$ electrolytes blocked with lithium electrodes are shown in

Figure 6 Electrochemical window of PVdF–HFP/SiO$_2$ electrolyte films prepared by (a) casting and (b) phase-inversion methods. The electrolyte solution was 1M LiPF$_6$ dissolved in EC/DMC (1:1 w/w).
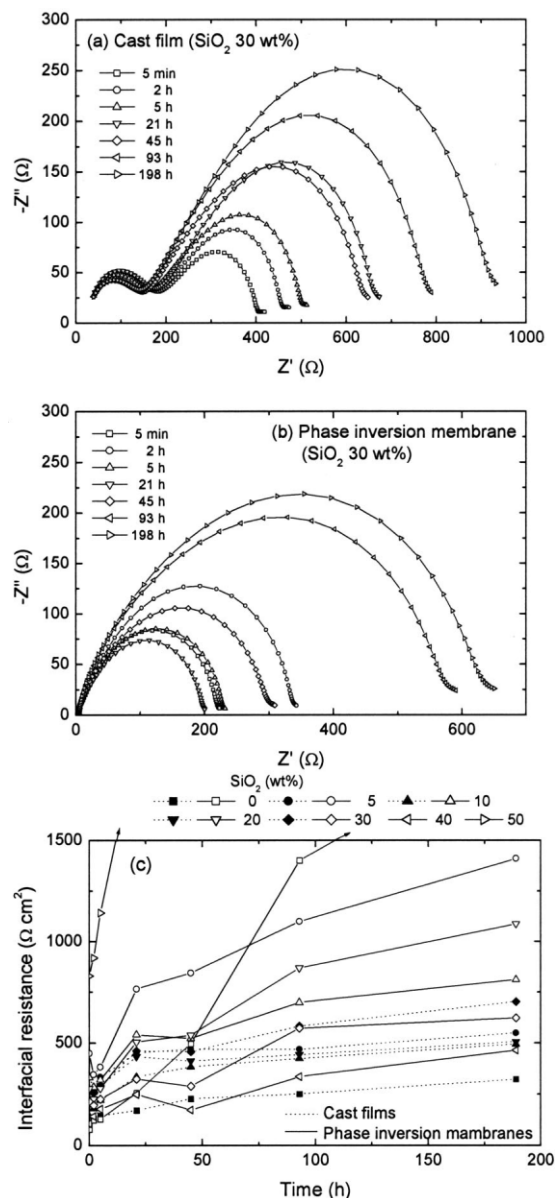
Figure 7 Impedance spectra of PVdF–HFP/SiO$_2$ (30 wt %) electrolytes prepared by (a) cast and (b) phase-inversion techniques on lithium electrodes as a function of time and (c) time evolution of the interfacial resistance between the polymer electrolyte and lithium electrodes. The electrolyte solution was 1M LiPF$_6$ dissolved in EC/DMC (1:1 w/w).

Figure 7(a,b) as a function of time. For the cast-film electrolytes, a small semicircle at a high frequency region, corresponding to the bulk resistance of the polymer electrolytes, is followed by a large semicircle at a low frequency, which is related to the interfacial resistance formed on the lithium electrode by the reaction with electrolyte components.[1,34] The bulk resistance is kept constant because of its compact structure with low porosity, but the interfacial resistance grows gradually with time. It seems that the growth of the interfacial resistance comes from the development of

an interfacial passivation layer formed between the bulk polymer electrolyte and lithium electrode. In contrast, the phase-inversion-membrane electrolyte showing just one semicircle seems to have the interfacial layer formed on the inner wall of large pores. Thus, the resistance contribution of the bulk-phase polymer electrolyte becomes sufficiently small to be neglected, although its bulk thickness is roughly 2–4 times higher than that of the cast films.

Figure 7(c) shows the time evolution of the interfacial resistance obtained from the impedance spectra. Comprehensively, the phase-inversion-membrane electrolytes yield higher interfacial resistance than the cast-film electrolytes, and this gets worse (increased resistance) with time. Fortunately, some phase-inversion samples with 30–40 wt % SiO$_2$ are comparable to cast samples in interfacial resistance. This is probably because they have a pore structure in which the growth of an interfacial passivation layer can be controlled to have a proper size, so that interfacial resistance no longer increases with time. More careful treatments will be needed to determine the control parameters accurately.

CONCLUSIONS

We report here the physical and electrochemical properties of PVdF–HFP/SiO$_2$ electrolytes prepared by casting and phase-inversion methods, mainly for use in rechargeable lithium batteries. Although the samples used in this work represent somewhat deviated properties with respect to the SiO$_2$ content, the phase-inversion samples are better than the cast samples according to the characterization results. Comprehensively optimizing such results, we have determined the phase-inversion PVdF–HFP/SiO$_2$ (20–30 wt %) polymer electrolytes to be best for application to rechargeable lithium batteries. On the other hand, it is also very significant to understand macro- and/or microscopic interactions occurring within the electrolyte membrane or film, in that those works essentially provide profound information on real polymer electrolyte properties. In this respect, more careful treatments and more precise conditions are needed for the phase-inversion polymer electrolytes to prove an accurate correlation between the conduction mechanism (carrier migration) and porous structure (porosity, pore size and distribution, pore connectivity, etc.).

References

1. Kim, K. M.; Ryu, K. S.; Kang, S.-G.; Chang, S. H.; Chung, I. J. Macromol Chem Phys 2001, 202, 866.
2. Kim, K. M.; Park, N.-G.; Ryu, K. S.; Chang, S. H. Polymer 2002, 43, 3951.
3. Kim, K. M.; Ko, J. M.; Park, N.-G.; Ryu, K. S.; Chang, S. H. Solid State Ionics 2003, 161, 121.

4. Boudin, F.; Andrieu, X.; Jehoulet, C.; Olsen, I. I. J Power Sources 1999, 81, 804.

5. Michot, T.; Nishimoto, A.; Watanabe, M. Electrochim Acta 2000, 45, 1347.

6. Kataoka, H.; Saito, Y.; Sakai, T.; Quartarone, E.; Mustarelli, P. J Phys Chem B 2000, 104, 11460.

7. Saito, Y.; Kataoka, H.; Sakai, T.; Deki, S. Electrochim Acta 2001, 46, 1747.

8. Magistris, A.; Mustarelli, P.; Quartarone, E.; Piaggio, P.; Bottino, A. Electrochim Acta 2001, 46, 1635.

9. Magistris, A.; Mustarelli, P.; Parazzoli, F.; Quartarone, E.; Piaggio, P.; Bottino, A. J Power Sources 2001, 97, 657.

10. Saito, Y.; Kataoka, H.; Quartarone, E.; Mustarelli, P. J Phys Chem B 2002, 106, 7200.

11. Magistris, A.; Quartarone, E.; Mustarelli, P.; Saito, Y.; Kataoka, H. Solid State Ionics 2002, 152, 347.

12. Jin, D. J.; Chang, C. L.; Huang, F. M.; Cheng, L. P. Polymer 2003, 44, 413.

13. Du Pasquier, A.; Warren, P. C.; Culver, D.; Gozdz, A. S.; Amatucci, G. G.; Tarascon, J.-M. Solid State Ionics 2000, 135, 249.

14. Capiglia, C.; Saito, Y.; Kataoka, H.; Komada, T.; Quartarone, E.; Mustarelli, P. Solid State Ionics 2000, 131, 291.

15. Saito, Y.; Kataoka, H.; Stephan, A. M. Macromolecules 2001, 34, 6955.

16. Huang, H.; Wunder, S. L. J Power Sources 2001, 97, 649.

17. Huang, H.; Wunder, S. L. J Electrochem Soc 2001, 148, A279.

18. Shi, Q.; Yu, M.; Zhou, X.; Yan, Y.; Wan, C. J Power Sources 2002, 103, 286.

19. Wang, T.; Xu, F.; Cheng, Y.; Jiang, Z. Chem Phys Lett 2002, 359, 303.

20. Stephan, A. M.; Saito, Y. Solid State Ionics 2002, 148, 475.

21. Quartarone, E.; Mustarelli, P.; Magistris, A. J Phys Chem B 2002, 106, 10828.

22. Saito, Y.; Stephan, A. M.; Kataoka, H. Solid State Ionics 2003, 160, 149.

23. Stephan, A. M.; Teeters, D. J Power Sources 2003, 119, 460.

24. Stephan, A. M.; Teeters, D. Electrochim Acta 2003, 48, 2143.

25. Bottino, A.; Camera-Rota, G.; Capannelli, G.; Munari, S. J Membr Sci 1991, 57, 1.

26. Welch, G. J.; Miller, R. L. J Polym Sci Polym Phys Ed 1976, 14, 1683.

27. Rosenberg, Y.; Sigmann, A.; Narkis, M.; Shkolnik, S. J Appl Polym Sci 1991, 43, 535.

28. Tazaki, M.; Wada, R.; Okabe, M.; Homma, T. J Appl Polym Sci 1997, 65, 1517.

29. Sajkiewicz, P. Eur Polym J 1999, 35, 1581.

30. Kim, K. M.; Jeon, W. S.; Park, N.-G.; Ryu, K. S.; Chang, S. H. Korean J Chem Eng 2003, 20, 934.

31. Marand, H. L.; Stein, R. S.; Stack, G. M. J Polym Sci Part B: Polym Phys 1988, 26, 1361.

32. Kim, K. M.; Kim, J.-C.; Ryu, K. S. Eur Polym J (submitted).

33. Kataoka, H.; Saito, Y.; Sakai, T.; Deki, S.; Ikeda, T. J Phys Chem B 2001, 105, 2546.

34. Appetecchi, G. B.; Croce, F.; De Paolis, A.; Scrosati, B. J Electroanal Chem 1999, 463, 248.